Published in final edited form as:
Neuropsychologia. 2012 October ; 50(12): 2812–2822. doi:10.1016/j.neuropsychologia.2012.07.042.

White matter fiber compromise contributes differentially to attention and emotion processing impairment in alcoholism, HIV-infection, and their comorbidity

T. Schulte[1,*], **E.M. Müller-Oehring**[1,2], **E.V. Sullivan**[1], and **A. Pfefferbaum**[1,2]

[1]SRI International, Neuroscience Program, 333 Ravenswood Ave, Menlo Park, California

[2]Department of Psychiatry and Behavioral Sciences, Stanford University, Stanford, California

Abstract

Alcoholism (ALC) and HIV-1 infection (HIV) each affects emotional and attentional processes and integrity of brain white matter fibers likely contributing to functional compromise. The highly prevalent ALC+HIV comorbidity may exacerbate compromise. We used diffusion tensor imaging (DTI) and an emotional Stroop Match-to-Sample task in 19 ALC, 16 HIV, 15 ALC+HIV, and 15 control participants to investigate whether disruption of fiber system integrity accounts for compromised attentional and emotional processing. The task required matching a cue color to that of an emotional word with faces appearing between the color cue and the Stroop word in half of the trials. Nonmatched cue-word color pairs assessed selective attention, and face-word pairs assessed emotion. Relative to controls, DTI-based fiber tracking revealed lower inferior longitudinal fasciculus (ilf) integrity in HIV and ALC+HIV and lower uncinate fasciculus (uf) integrity in all three patient groups. Controls exhibited Stroop effects to positive face-word emotion, and greater interference was related to greater callosal, cingulum and ilf integrity. By contrast, HIV showed greater interference from negative Stroop words during color-nonmatch trials, correlating with greater uf compromise. For face trials, ALC and ALC+HIV showed greater Stroop-word interference, correlating with lower cingulate and callosal integrity. Thus, in HIV, conflict resolution was diminished when challenging conditions usurped resources needed to manage interference from negative emotion and to disengage attention from wrongly cued colors (nonmatch). In ALC and ALC+HIV, poorer callosal integrity was related to enhanced emotional interference suggesting curtailed interhemispheric exchange needed between preferentially right-hemispheric emotion and left-hemispheric Stroop-word functions.

Keywords

DTI-based fiber tractography; attention; emotion; HIV infection; alcoholism

*Correspondence Tilman Schulte, Ph.D. SRI International 333 Ravenswood Avenue Menlo Park, CA 94025-3493 Phone: 650-859-2767 FAX: 650-859-2743 tilman.schulte@sri.com.

There are no financial or other relationships that could be interpreted as a conflict of interest affecting this manuscript.

1. Introduction

A substantial proportion of individuals with HIV have comorbid conditions, notably alcohol abuse (Cooper & Cameron, 2005), which can impair immune responses possibly exacerbating neuroinflammation and neurodegeneration (Persidsky et al., 2011; Potula et al., 2006). Alcohol consumption is also associated with an increase in HIV type 1 virus replication in peripheral blood mononuclear cells (Bagasra & Pomerantz, 1993) and compromise of the blood brain barrier, thereby increasing viral entry and microglial activation (Persidsky et al., 2000; Wang, Sun, & Goldstein, 2008). There is evidence that both HIV-1 and alcohol induce oxidative stress by enhancing the production of cytotoxins associated with neuronal compromise (Boyadjieva & Sarkar, 2010; Gonzalez-Scarano & Martin-Garcia, 2005) and targets gene expression level associated with defects in myelin metabolism and HIV-1-associated neurocognitive disorder (Borjabad et al., 2011).

Functional and structural neuroimaging studies in HIV (Ernst, Chang, Jovicich, Ames, & Arnold, 2002) and in alcoholism (Fein et al., 2006; Makris et al., 2008; Marinkovic et al., 2009) report abnormalities in frontostriatal and limbic systems, which are relevant for emotional and reward processing and for cognitive and behavioral control. The caudate is preferentially affected in HIV (Ances et al., 2006; Goodkin et al., 1997) and is associated with gating functions of salient and emotionally relevant information (Carretie et al., 2009; Horvitz, 2002) and with reward-based behavioral learning (Haruno et al., 2004; Kim and Lee, 2011). HIV and alcoholism each also affect gray matter nodes of limbic and frontal brain systems (HIV: Ances et al., 2012; Clark, Cohen, Westbrook, Devlin, & Tashima, 2010; Di Sclafani et al., 1997; Stout et al., 1998; Towgood et al., 2012; alcoholism: Fortier et al., 2011; Pfefferbaum et al., 2012) as well as white matter fibers connecting subcortical and cortical nodes (HIV: Gongvatana et al., 2011; Pfefferbaum et al., 2009; alcoholism: Pfefferbaum, Rosenbloom, Fama, Sassoon, & Sullivan, 2010; Rosenbloom, Sullivan, & Pfefferbaum., 2003; Schulte, Müller-Oehring, Rohlfing, Pfefferbaum, & Sullivan, 2010).

Limbic circuits involving prefrontal, medial temporal, and the cingulate cortices have been associated with processing emotion and attention (Etkin, Egner, & Kalisch, 2011; Schulte Müller-Oehring, Sullivan, & Pfefferbaum, 2012). The uncinate fasciculus (*uf*) and the cingulum (*c*) connect these regions, and degradation of fiber integrity in these bundles may influence transfer of information among regions intercepting these limbic circuits (Zhang et al., 2012). Lateral frontal, temporal and parietal cortices play a key role for selective attention and executive control and are interconnected by superior (*slf*) and inferior longitudinal fasciculus (*ilf*) (Yin et al., 2011). Emotion functions are preferentially processed in the right cerebral hemisphere (Adolphs, Damasio, Tranel, & Damasio, 1996; Hartikainen Ogawa, & Knight, 2000) and verbal functions in the left cerebral hemisphere, recently confirmed with functional imaging for Stroop-word conflict processing (Schulte et al., 2012). The corpus callosum, the thick band of white matter fibers connecting cortices of the two cerebral hemispheres, enables interhemispheric transfer of information (Barnett & Corballis, 2005; Barrick, Lawes, Mackay, & Clark, 2007; Schulte et al., 2010) pertinent to cognitive control (Schulte, Müller-Oehring, Javitz, Pfefferbaum, & Sullivan, 2008). Thus, the deleterious effect of both HIV infection and alcohol abuse on cortical and subcortical interconnected circuits including mesocorticolimbic pathways from brain stem nuclei (substantia nigra, ventral tegmental area) to basal ganglia and cortices (Koob, 2011; Kumar, Ownby, Waldrop-Valverde, Fernandez, & Kumar, 2011) could result in impairment in attention, and executive functions (Fama, Rosenbloom, Nichols, Pfefferbaum, & Sullivan, 2009; Fama et al., 2011; Martin et al., 2007; Schulte, Mueller-Oehring, Rosenbloom, Pfefferbaum, & Sullivan, 2005) and emotional dysregulation (Johnson-Greene, Adams, Gilman, & Junck, 2002; Salloum et al., 2007; Schulte et al., 2011). Although the fiber bundles connecting key cortical regions involved in processing emotion, attention, and

cognitive control are well known, the roles of cortico-limbic and callosal fiber integrity for emotional and attentive control are not yet established in HIV and alcoholism.

In search of brain substrates of emotional and attentional dysregulation, we used MR diffusion tensor imaging (DTI) and quantitative fiber tracking of selective association brain fiber tracts in patients with alcoholism, HIV infection, or comorbidity for both condition. DTI yields fractional anisotropy (FA), a measure of the degree to which water diffusion exhibits a predominant orientation: the more linear and organized the fibers in a region, the higher the FA and the lower the diffusivity (Basser & Jones 2002; Mori & Zhang, 2006). Thus, FA and diffusivity provide measures of the microstructural integrity of local fiber bundles including a metric sensitive to the condition of myelin ([notdef]t, transverse diffusivity). We used an emotional Stroop Match-to-Sample task and added a cueing component to the task because this enabled emotion, attention and executive control to be tested separately (Bannerman, Milders, & Sahraie, 2010). Our task, which required subjects to match the color of a cue to that of an emotional word, showed that HIV patients with or without alcoholism and patients with alcoholism alone have greater difficulty than controls in resolving conflict arising from emotional words (Schulte et al., 2011).

Here, we sought to identify brain substrates of these attention and emotion functions. We hypothesized that 1) deficits in emotion processing would be related to disruption of uncinate fasciculus (*uf*) and cingulum (*c*) fiber tracts; 2) deficits in attention and conflict resolution to inferior (*ilf*) and superior longitudinal fasciculi (*slf*); and deficits in integrating right-lateralized emotion and left-lateralized Stroop word processes to corpus callosum (*cc*) integrity (Schulte et al., 2012) in patients with either HIV-infection or alcoholism. Patients with both disorders would show the greatest compromise and relations observed in each condition alone.

2. Methods

2.1. Participants

Behavioral data were taken from our earlier study (Schulte et al., 2011) and included participants who also had DTI data acquired contemporaneously. The four participant groups were comprised of: 19 patients with alcoholism alone (ALC), 16 patients with HIV-1 infection alone (HIV), 15 patients with ALC+HIV comorbidity, and 15 healthy controls (CTL). All participants gave written informed consent to participate in the study, which was approved by the institutional review boards at Stanford University School of Medicine and SRI International. All volunteers were screened by trained clinicians using the Structured Clinical Interview for DSM-IV (American Psychiatric Association, 1994) to exclude schizophrenia, bipolar disorder, current (past 3 months) non-alcohol drug abuse or dependence, or use of drugs (excluding cannabis and tobacco) in the past month. Healthy control participants did not meet criteria for any lifetime Axis I pathology. Medical exclusions were head trauma, documented compound skull fracture, clear neurologic sequelae, or any disease with potential central nervous system involvement, such as stroke, multiple sclerosis, or epilepsy. The study groups did not differ in age, gender or verbal intelligence (ANART IQ, National Adult Reading Test; Nelson, 1982) (Table 1). All subjects were right handed as determined with a quantitative questionnaire (Crovitz & Zener, 1962).

Lifetime alcohol consumption (in kilograms) was estimated using a semistructured interview (Pfefferbaum, Rosenbloom, Crusan, & Jernigan, 1988). Drinks of each type of alcoholic beverage were standardized to units containing approximately 13.6g of alcohol and summed over the lifetime. Groups differed significantly in lifetime alcohol consumption, with the two alcohol groups having consumed significantly more alcohol than the control and the

HIV group, whereas ALC and ALC+HIV groups did not significantly differ from each other (Tab. 1). The two alcoholism groups did not differ in length of alcohol abstinence prior to study participation, and age at onset of alcoholism. Longer alcohol abstinence was associated with higher amounts of lifetime alcohol consumption in ALC+HIV (*rho*=.47, *p*=.046). The two HIV groups did not differ in age at onset of HIV-1 infection. Among the 15 subjects in the ALC+HIV group, alcoholism preceded HIV-1 infection in 12 subjects, and HIV-1 infection preceded alcoholism in 2 subjects. Onset of alcoholism was unknown in one woman. The HIV and ALC+HIV groups did not differ in CD4 T-cell count, an index of disease severity (Tab. 1).

The Karnofsky scale, which ranged from 0 to 100 (Karnofsky, Abelmann, Craver, & Burchenal, 1948), characterized each patient's HIV-infection disease severity in terms of daily functioning; no one scored below 80 (normal activity with effort and some signs of disease), 10% were scored 90 (normal activity; minor signs of disease), and 90% had no evidence of significant functional compromise (score 100). Regarding HIV medication, 81% in the HIV group and 87% in the ALC+HIV group were taking highly active antiviral treatment (HAART). There was no significant difference in medication status between these two study groups (Tab. 1).

To address the potential contribution of depressive symptoms to our primary dependent measures, we used the Beck Depression Inventory (BDI-II), a quantitative measure of depressive symptoms (Beck, Steer, & Brown 1996). BDI scores of 0–13 indicate minimal, 14–19 mild, 20–28 moderate, and 29–63 severe depressive symptoms. HIV and ALC+HIV groups scored on average within the minimal, non-clinical range. The scores were even lower for alcoholics and lowest in healthy controls. Groups differed significantly in BDI scores (Tab. 1); however, over all groups BDI-estimated depression was minimal. In the ALC+HIV group higher BDI scores correlated moderately with higher amounts of lifetime alcohol consumption (kg) (*rho*=.47, *p*=.046). DSM-IV diagnoses assigned at the SCID interview indicated that 2 ALC patients met criteria for current major depression, and 5 ALC, 3 HIV and 5 ALC+HIV had met depression criteria in the past (full remission). In addition, 3 HIV and 6 ALC+HIV tested positive for Hepatitis-C infection (HCV); 5 ALC and 4 ALC+HIV had also used other drugs than alcohol including cocaine, opioids, and amphetamines within the past year but not within the past 3 months prior to testing. One CTL, 8 ALC, 3 HIV and 7 ALC+HIV were current smokers and 2 ALC, 2 HIV and 1 ALC +HIV past smokers. Together, 7 ALC, 4 HIV, and 10 ALC+HIV had at least one other comorbidity, including mood disorder. Finally, all subjects took a breath-alcohol analyzer test to ensure abstinence from alcohol at the time of testing.

2.2. Data Acquisition and Analyses

The emotional Stroop Match-to-Sample task required subjects to match the color of targets, an emotional word (HAPPY, ANGRY) or a letter string (XXXXX) printed in red, green, or blue to that of a prior color cue (Fig. 1). Cue and target colors matched in half of the trials. Participants pressed a YES-key for color matches and a NO-key for color nonmatches.

In the color match `*baseline*' condition, the target stimulus consisted of the neutral letter string XXXXX. In the color match `*emotional word*' condition, the target stimulus consisted of the word HAPPY or the word ANGRY. Stroop color-word conflict was defined as interference from the word's content while matching cue and word ink colors, and calculated by subtracting color matching times for letter string trials (baseline) from those for word trials, separately for positive (HAPPY – XXXXX) and negative (ANGRY – XXXXX) emotional words.

In half of the color match trials, an emotional *face cue* (happy or angry faces) was presented between *color cue* and *target* stimulus to test how an emotional face would influence color matching per se and conflict resolution for emotional Stroop words. Emotional face cues were presented in combination with a letter string, i.e., `happy face–XXXXX' and `angry face–XXXXX' and in combination with emotional Stroop words. In these `*face+word*' trials, facial expression and Stroop word content always conveyed the same emotion, i.e., `happy face–word HAPPY' and `angry face–word ANGRY.'

Conditions were administered in blocks of 4 trials; blocks were presented in pseudo-random order thereby ensuring the same number of trials per condition for each subject. In total, 96 trials were presented with 24 trials in each of the four color-match conditions: 1) no face–letter string, 2) no face–emotional word, 3) face cue–letter string, and 4) face cue–emotional word. Number of correct responses, errors and reaction time data were recorded for each trial and subject. Subjects had to make at least 80% correct responses to be included for further analyses.

2.3. Diffusion Tensor Imaging

2.3.1. DTI and MRI Acquisition—All imaging data were acquired with an 8-channel head coil at 3T after higher-order (nonlinear) shimming (Kim, Adalsteinsson, Glover, & Spielman, 2002). DTI and fast spin echo (FSE) structural data were collected with the same slice locations: DTI (2D echo-planar, TR=7300ms, TE=86.6ms, thickness=2.5mm, skip=0, locations=62, b=0 (5 NEX)+15 noncollinear diffusion directions b=860s/mm^2 (2 NEX)+15 opposite polarity noncollinear diffusion directions b=860s/mm^2 (2 NEX), FOV=240mm, xdim=96, y-dim=96, reconstructed to 128×128, 4030 total images); FSE (2D axial, TR=7850ms, TE=17/102ms, thickness=2.5mm, skip=0, locations=62). The dual-echo FSE sequence acquired as part of the DTI protocol was used for co-registering structural and diffusion images. T1-weighted SPGR (3D axial IR-prep, TR=6.5ms, TE=1.6ms, thick=1.25mm, skip=0, locations=124) images were aligned, such that two 1.25mm SPGR slices subtended each 2.5mm-thick FSE/DTI slice. A field map was generated from a gradient recalled echo sequence pair (TR-460ms, TE=3/5ms, thickness=2.5mm, skip=0mm, locations=62).

2.3.2. DTI Analysis—DTI quantification was preceded by eddy-current correction on a slice-by-slice basis using within-slice registration, which took advantage of the symmetry of the opposing-polarity acquisition (Bodammer, Kaufmann, Kanowski, & Tempelmann, 2004) and also allowed for compensation of the diffusion effect created by the imaging gradients (Neeman, Freyer, & Sillerud, 1991), reducing the data to 15 non-collinear diffusion-weighted images per slice for tensor computation. Using the field maps, B0-field inhomogeneity-induced geometric distortion in the eddy current-corrected images was corrected with PRELUDE (Phase Region Expanding Labeller for Unwrapping Discrete Estimates, Jenkinson, 2003) and FUGUE (FMRIB's Utility for Geometrically Unwarping EPIs, Jenkinson, 2001).

DTI models water diffusion within each voxel as a zero-mean multivariate Gaussian distribution, which is parameterized by its symmetric 3×3 covariance matrix, the diffusion tensor. The diffusion-weighted data measured with respect to each of the diffusion gradient directions exhibits a signal attenuation relative to b=0 data acquired without diffusion gradients. The logarithm of this signal attenuation is a linear combination of the six unique elements of the diffusion tensor, their weights determined by the direction of the diffusion gradients. Computing a least squares solution for this over-determined linear equation system independently at each voxel yielded the elements of the diffusion tensor for that voxel. The diffusion tensor was then diagonalized to obtain eigenvalues $\lambda 1$, $\lambda 2$, $\lambda 3$, and

corresponding eigenvectors. From the eigenvalues, fractional anisotropy (FA) and two orientational diffusivity measures, λl and λt, were calculated on a voxel-by-voxel basis (Basser & Jones, 2002; Basser & Pierpaoli, 1998; Pierpaoli & Basser, 1996). These "native space" DTI data were also used for fiber tracking.

A diffusion tensor can be graphically represented by an equidensity ellipsoid. The axes of this ellipsoid are oriented according to the eigenvectors of the tensor, and their lengths are proportional to the square roots of the corresponding eigenvalues. In tissue that is highly linear, one eigenvalue dominates the other two. The ellipsoid is, therefore, long and narrow and has a preferential orientation, presumed to indicate the course of white matter fiber tracts. FA quantifies the degree to which water diffusion exhibits a predominant orientation: the more linear and organized the fibers in a region, the higher the FA. In an ellipsoid with a preferential orientation, its long axis is referred to as longitudinal, or axial, diffusivity (λl = λ1), which has been shown to be an indicator of axonal integrity. The mean of the short axes of the diffusion ellipsoid is referred to as transverse, or radial, diffusivity (λt = [λ2 +λ3]/2), which is considered a marker of myelin integrity (Song et al. 2002; Sun et al. 2006).

2.3.3. Fiber Bundle Identification and Tracking—Fiber tracking was performed with the software by Gerig et al. (2005) based on the method of Mori and colleagues (Mori & van Zijl, 2002; Xu, Mori, Solaiyappan, van Zijl, & Davatzikos, 2002; Xue, van Zijl, Crain, Solaiyappan, & Mori, 1999). This approach requires the identification of a group of "source" voxels from which streamlines (i.e., fiber tracts) are initiated and propagated throughout the brain following the orientation of the principal eigenvector of the diffusion tensor at each point along the fiber. To describe a particular fiber bundle selectively, a group of "target" voxels is also identified, and only the streamlines that pass through the target are retained. Thus, each identified fiber bundle is required to originate in a source voxel and pass through at least one target voxel.

Fiber tract sources and targets were identified on the FA image of the SRI24 atlas (Rohlfing, Zahr, Sullivan, & Pfefferbaum, 2010; http://nitrc.org/projects/sri24) as follows. The major targets for the commissural tracts were identified as all voxels of the corpus callosum in the midsagittal slice. They were then divided into seven sectors, reflecting divisions determined with histological analysis (Pandya & Seltzer, 1986). Commissural sources were two 3-mm-thick planes, 5mm bilateral to commissural targets. The uncinate fasciculus and the superior and inferior longitudinal fasciculi were identified in the middle of their extent. The cingulate bundle was identified in three sections: superior, posterior, and inferior. The midpoint voxel of each fasciculus and each cingulate section was dilated with a morphological operator to produce a 5mm cube as the fiber tracking target. Sources were 3mm-thick planes placed 5mm anterior and 5mm posterior to the targets.

These targets and sources were mapped to the corresponding locations on the native-space DTI images for each subject using coordinate transformations computed by nonrigid image registration (Rohlfing & Maurer, 2003; http://nitrc.org/projects/cmtk/). In particular, the SPGR channel of the SRI24 atlas was registered to each subject's SPGR image, which was registered to that subject's FSE image pair, which in turn was registered to the *b*=0 image of the subject's DTI acquisition. All three transformations were concatenated to produce sources and targets in the subject's DTI space using only a single reformatting operation.

The tensor data as well as targets and sources were passed to the fiber tracking routine in native space, thus avoiding the need for tensor field resampling and tensor reorientation. Fiber tracking parameters included white matter extraction threshold (minimum FA) of .17, minimum fiber length of 37.5 mm, maximum fiber length of 187.5 mm, fiber tracking threshold of .125 (terminates a fiber if the vector field in the local neighborhood is too

noisy), and angle of maximum deviation of .80 (~37° maximum angle between successive fiber segments). In postprocessing, we enforced the additional constraint that a commissural fiber originating in a source voxel in one hemisphere was required to pass through a target voxel in the corpus callosum and also through at least one source voxel in the other hemisphere.

The output of the fiber tracking for each subject and each source-target pair was a 3D geometric model of the fiber paths comprising a table of all point locations along each fiber with local DTI metrics (FA, MD, λ1, λ2, λ3). Mean FA, longitudinal diffusivity (λl = λ1), and transverse diffusivity (λt = [λ2 + λ3]/2) for each fiber bundle were the units of subsequent analysis.

2.4. Statistical Analyses

For behavioral data analysis, mean reaction times (RTs) for correct YES and NO responses and the numbers of errors were computed for each subject for each color-match condition. For the analyses of specific task effects, we calculated *Stroop* effects for positive and negative emotional words as the difference in reaction time (RT) between word and letter string trials for both color match and nonmatch trials and separately for trials with and without face cues.

For DTI fiber microstructural analysis, we used MANOVAs to test for group differences in FA, λl, and λt in each fiber bundle. Significant group effects were followed up with post-hoc Least Square Difference (LSD) tests. To examine the relationships between fiber integrity (FA), emotion and conflict processing within each group, we used non-parametric Spearman Rho correlation analyses. Finally, to test for relationships between DTI fiber microstructure, demographic and clinical variables and performance, we used Spearman Rho correlation (one-tailed), based on the assumption that less fiber integrity and higher severity of illness would result in poorer performances (slower processing speed, more errors). Applying family-wise Bonferroni correction for comparisons of 7 DTI fiber tracts, p-values ≤ .014 (1-tailed) and p-values ≤ .007 (2-tailed) were considered significant. For all other statistical tests, alpha significance levels were set at $p<.05$, 2-tailed (SPSS 15.0).

3. Results

3.1. Behavioral Performance

3.1.1. Accuracy—The four groups did not differ significantly in number of errors committed ($F(3,61)=1.67$, $p=.09$; $\eta^2_p=.08$), although, on a descriptive level, ALC+HIV (8±6 errors) and HIV (7±5 errors) committed more errors than CTL (5±3 errors) or ALC (5±4 errors). Number of errors and overall reaction times (RTs) were not significantly correlated in CTL, HIV, and ALC+HIV groups, and the positive correlation in ALC ($r=.50$, $p<.03$; $Rho=.44$, $p=.06$) indicated lack of speed-accuracy trade off.

3.2. Attention, Emotion, and Conflict Processing

3.2.1. Attention and emotional faces—A repeated-measures ANOVA testing for effects of attentional color cueing (match, nonmatch) and emotional faces (no face, happy face, angry face) in letter string trials (XXXXX) as within-subjects factor and group as between-subjects factor (CTL, ALC, HIV, ALC+HIV) showed that all groups (group effect and interactions, p's > .05) had longer RTs to nonmatch than match trials ($F(1,61)=88.37$, $p<.0001$) and to trials with angry than happy faces that were longer than RTs to trials with no faces (face effect: $F(1,61)=19.56$, $p<.0001$; attention-by-face interaction: $F(1,61)=10.07$, $p=.002$) (Figure 2A).

3.2.2. Emotion and Stroop conflict—We next tested whether groups differed in Stroop conflict depending on the emotional content of the Stroop word and the presence of an emotional face. To control attention effects, we tested this separately for match (valid color cue) and nonmatch (invalid color cue) trials by using repeated-measures ANOVAs with Stroop words (word/no word), faces (face/no face) and emotional content (happy/angry) as within subject factors and group (CTL, ALC, HIV, ALC+HIV) as between subjects factor.

For *match* trials, groups differed significantly in the interaction between emotional Stroop and emotional face effects (group-by-emotional Stroop-by-face interaction: $F(1,61)=13.95$, $p=.021$) (Fig. 2B). Overall, Stroop effects were greater for emotionally negative (ANGRY) than positive (HAPPY) words (emotional Stroop effect: $F(1,61)=9.44$, $p=.003$). Follow-up analyses revealed a significant group effect ($F(3,61)=3.80$, $p=.015$) showing enhanced Stroop interference from the word HAPPY (no faces) in HIV ($p=.032$) and ALC+HIV ($p=.003$) relative to controls, who did not show Stroop interference on trials without faces (Fig. 2B). In addition, within group follow-up analyses revealed an emotional Stroop-by-face interaction in CTL ($F(1,14)=6.18$, $p=.026$), illustrating that Stroop effects for positive emotion was enhanced by presenting happy faces, while the overall greater Stroop effect for negative emotion was barely modulated by angry faces. Also, ALC showed greater Stroop effects for negative than positive emotional words ($F(1,18)=4.42$, $p=.05$), but these were not significantly modulated by emotional faces (interaction: $F(1,18)=1.24$, *ns*). Patients with HIV alone did not show any significant modulation of Stroop-match effects by emotional word content and emotional faces (all p's>.05). In contrast to the pattern observed in controls, those with comorbid ALC+HIV tended to show enhanced Stroop conflict (for ANGRY) for angry faces and reduced Stroop conflict (for HAPPY) for happy faces (emotional Stroop-by-face interaction: $F(1,14)=4.52$ $p=.058$) (Fig. 2B).

For *nonmatch* trials, groups did not differ in emotional Stroop effects (group main and interaction effects, p's>.05). Also here, Stroop effects were greater for negative (ANGRY) than positive (HAPPY) emotional words (emotional Stroop effect: $F(1,61)=21.6$, $p<.0001$), and for trials with than without emotional faces ($F(1,61)=16.1$, $p<.0001$), especially when the Stroop word `ANGRY' was preceded by an angry face (emotional Stroop-by-face interaction: $F(1,61)=5.23$, $p=.026$) (Fig. 2B). However, between group analyses for each Stroop effect separately (HAPPY-no face; HAPPY+face; ANGRY-no face; ANGRY+face) revealed a trend for a group effect ($F(3,61)=2.63$, $p=.058$) showing enhanced Stroop-ANGRY word interference (trials without faces) in ALC+HIV compared to controls ($p=.009$) (Fig. 2B).

3.3. Brain Microstructure

To test for group differences (CTL, HIV, ALC, HIV+ALC) in brain microstructure, MANOVAs were applied to each measure of fiber integrity (FA, λt, λl) and for the superior (*slf*) and inferior longitudinal fasciculus (*ilf*), cingulum (superior (*sc*), posterior (*pc*) and inferior (*ic*), uncinate fasciculus (*uf*), and corpus callosum (*cc*) fiber tracts. The results are summarized in Tab. 2. Relative to CTL, DTI-based fiber tracking revealed lower FA in *ilf* and *uf* in all three patient groups (p's<.05). Transverse diffusivity (λt) in the *uf* was greater in HIV and ALC+HIV than in CTL (Tab. 2).

3.4. Correlation Analyses

3.4.1. Fiber integrity and performance—Tab. 3 summarizes the results of the DTI-Stroop correlations. In CTL, longer Stroop-nonmatch effects for negative emotional words (ANGRY) were related to higher cingulum (*pc*) diffusivity (λt, λl). However, when the emotional Stroop word HAPPY was primed by a happy face, greater Stroop-nonmatch

effects were related to higher integrity (higher FA, lower λt, λl) of the inferior longitudinal fasciculus (*ilf*), cingulum (*sc*), and corpus callosum (*cc1, cc2, cc3, cc5*).

In ALC, only for trials with facial cueing, greater Stroop effects (for ANGRY and HAPPY) were related to lower fiber integrity mainly in the cingulum (*sc*) and for nonmatch trials additionally to callosal (*cc3, premotor*) fiber integrity. In HIV, greater Stroop-ANGRY effects for nonmatch trials were related to lower fiber integrity in the uncinate fasciculus (*uf*). In ALC+HIV, greater Stroop-ANGRY effects for nonmatch trials and with `angry face' cues were related to lower callosal (*cc5, sensory*) fiber integrity.

3.4.2. Fiber integrity, age and clinical measures—Tab. 4 summarized the results of the correlation analysis.

3.4.2.1. Age: In the healthy control group, older age was related to higher diffusivity in the inferior longitudinal fasciculus (*ilf*) fiber bundle. Similarly, in alcoholics older age was related to lower fiber integrity in the *ilf* and additionally in the cingulum (*sc*) and uncinate fasciculus (*uc*). Older age was only moderately correlated with higher callosal diffusivity in HIV (*cc5* λ*t:rho*=.47, *p*=.035; *cc5* λ*l:rho*=.48, *p*=.032) and ALC+HIV (*cc6* λ*t:rho*=.51, *p*=.027).

3.4.2.2. Alcohol consumption parameters: In the comorbid ALC+HIV group, longer periods of alcohol abstinence before testing were related to higher callosal FA in the parietal sector (*cc6*) (Tab. 4) and moderately with other callosal sectors (*cc4:rho*=.45, *p*=.047; *cc7*: *rho*=.53, *p*=.021) and the cingulum (*pc:rho*=.55, *p*=.016). In ALC, only a moderate correlation was found between higher amounts of lifetime alcohol consumption and lower *slf* FA (*rho*=.45, *p*=.029).

3.4.2.3. CD4 t-cell count: Moderate relationships were further observed between higher CD4 cell counts and higher corpus callosum FA in HIV (for *cc1, rho*=.44, *p*=.046) and between CD4 count and callosal (for *cc7,rho*=.45, *p*=.046) and cingulum FA (*pc*) in ALC+HIV (*rho*=.55, *p*=.016).

3.4.2.4. Overall performance: In both HIV groups, lower callosal fiber integrity was predictive of slower processing speed (HIV: *cc5*; ALC+HIV: *cc3*, *cc5*) (Tab. 4). Lower accuracy (more errors) was related to lower *uf* integrity in HIV and lower *slf* integrity in ALC+HIV (Tab. 4).

4. Discussion

The focus of this study was to examine whether attentional and emotional processes were associated with microstructural integrity of regional fiber systems in patients with HIV-1 infection with or without alcoholism and those with alcoholism alone. Consistent with earlier studies, all groups had longer reaction times to nonmatch than match trials, because nonmatch trials are assumed to usurp processing resources due to the mismatch of the color cue and color naming of the word (Schulte et al., 2005; Schulte et al., 2011; Williams, Mathews, & MacLeod, 1996). Response times were longer for angry than happy faces, indicating that more resources were needed to process negative emotion (Huang et al., 2011), an effect that was similar in all groups. Despite similar baseline color-matching performance for trials with and without emotional faces, however, the groups differed on Stroop conflict processing, especially for match trials. Here, HIV and ALC+HIV showed greater Stroop interference for positive emotional words than controls. Overall, emotional face presentation enhanced emotional Stroop effects. While in controls, this enhancement was observed specifically for positive emotion, emotional faces regardless of valance did not

modulate Stroop effects in patients with ALC or HIV alone. In the comorbid ALC+HIV group, this enhancement was observed for negative rather than positive emotion. Under attentionally more challenging nonmatch conditions, the comorbid ALC+HIV group showed the greatest Stroop interference from negative emotion relative to all groups. This greater Stroop conflict for negative emotion and the observed increases of Stroop conflict with negative facial stimuli may indicate difficulties with emotional processing in patients with ALC+HIV (Hutton et al., 2004).

Similar to previous reports of compromised fiber integrity in HIV infection (Chang et al., 2008; Laubenberger et al., 1996; Pfefferbaum et al., 2009) and alcoholism (Pfefferbaum et al., 2010; Schulte et al., 2005; Wang et al., 2009), we found that relative to controls, all three patient groups (HIV, ALC and ALC+HIV) had lower fractional anisotropy, in particular in the inferior longitudinal fasciculus (*ilf*) (connecting frontal and posterior attentional regions) and uncinate fasciculus (*uf*) (connecting frontal to limbic emotional regions). The cingulum and uncinate fascilulus are part of the cortico-striatal-limbic circuit involved in processing emotional stress, alcohol cues, and reward (Seo, Barraclough, & Lee, 2011). The anatomical characteristics of the underlying white matter tracts, and associated axonal injury or impaired conductivity (Kumar & Cook, 2002), can be a marker of compromised neural connectivity in cortico-cortical and cortico-subcortical circuits and potentially subserve functional dysregulation of emotion and cognition (Schulte et al., 2011). For example, Zhang et al. (2012) recently reported that the severity of depression was associated with microstructural abnormalities in the uncinate fasciculus.

Having found regional white matter compromise in several fibers, we analyzed structure-function relationships between fiber integrity and performance in patients with HIV and alcoholism. Attentional challenge (color nonmatch) and negative emotional content during Stroop processing both revealed the relevance of fiber integrity in all groups, but the fiber connectivity tracts for functional modulation differed between groups. In controls, the amount of Stroop conflict elicited by an emotional word was predicted by fiber integrity in several fiber bundles, including the inferior longitudinal fasciculus and cingulum (*sc*, *pc*), and the corpus callosum (*cc1–3*, *cc5*) when emotional words were primed by face cues. Also in alcoholics, Stroop-word conflict with face cueing was related to callosal (*cc3*) and cingulum (*sc*) fiber integrity, and in comobid ALC+HIV patients to callosal sensory sector integrity (*cc5*). In patients with HIV alone, greater interference from negative Stroop-words was related to lower uncinate fasciculus integrity.

The differential fiber tracts in the two HIV groups may suggest different underlying processes: Uncinate fasciculus microstructure was compromised in the HIV relative to controls, and this compromise may have contributed – at least in part – to poorer conflict resolution when challenging conditions usurp resources needed to curtail interference from negative emotion and to disengage attention from the wrongly cued color during nonmatch (Rochat, Billieux, & Van der Linden, 2011). Although structure-function relationships were observed mostly for color-nonmatch trials; in alcoholics, we found relationships also for attentionally less challenging color-match conditions. In this case, lower superior cingulum fiber integrity was related to enhanced word interference, especially when the emotional content of the word was cued by an emotional face. Thus, in alcoholics, fiber integrity modulated processing of emotional content during both, more and less attentionally challenging conditions. We speculate that variability in cingulum fiber integrity may help synchronization of neural communication between limbic emotion and frontoparietal attention systems needed to control intrusion of emotional information during color matching. In ALC+HIV, the posterior callosal region was associated with poorer conflict resolution for negative emotion in nonmatch trials; here, cueing from the additional `angry face' may have necessitated interhemispheric exchange of information to resolve Stroop

conflict, preferentially processed in the left hemisphere (Schulte et al., 2012), and interference from angry faces, which are preferentially processed in the right hemisphere (Jackson, Wolf, Johnston, Raymond, & Linden, 2008). Callosal involvement for Stroop conflict processing was further observed in controls and alcoholics, and again only for trials with emotional face cues. While this structure-function relationship was compromise-oriented in the patient groups, i.e., lower callosal integrity was related to greater Stroop-word interference for trials with emotional face cues, this was not the case in controls. Controls showed Stroop effects for positive emotional content only when the word HAPPY was cued by a happy face, i.e., evidence that the word's emotional content was actually processed, and this normal Stroop interference was related to better fiber integrity. Together, these results support the assumption that the corpus callosum plays a role in integrating preferentially lateralized processes of nonverbal emotional interference and verbal Stroop conflict resolution (Silveri et al., 2006).

There is evidence for differential neurobiological substrates for processing positive and negative emotion. For example, a recent ERP study reported that unpleasant emotion, but not pleasant emotion, influenced the early stage of behavioral inhibitory control by enhancing the monitoring of response conflicts (Wang et al., 2011). In the current study, we also found differential effects for negative and positive emotion in controls, who showed interference from the word ANGRY, whereas for the word HAPPY interference was only observed when it was cued by a happy face. Here, greater interference from positive emotion was related to higher callosal fiber integrity, possibly allowing faster interhemispheric communication between preferentially right-hemispheric facial and left-hemispheric word processes. By contrast, lower integrity in several fiber tracts correlated with enhanced interference from negative emotion, particularly during color-nonmatch conditions. These findings support the assumption of different neurobiological substrates for positive and negative emotion with enhanced alerting for negative emotion (Yuan et al., 2007) and relatively less biological significance for pleasant stimuli for self-preservation (Wang et al., 2011; Yuan et al., 2011). Moreover, different neurotransmitter systems seem to be involved in processing positive and negative emotional expressions (Blair, 2003): Serotonergic manipulations differentially affected the processing of fearful and happy expressions (Harmer et al. 2001), and dopaminergic and GABAergic manipulations differentially affected the processing of angry expressions (Borrill et al. 1987; Blair & Curran 1999; Zangara et al. 2002). Together, our results complement findings on different neurobiological substrates for positive and negative emotion by showing that in the healthy brain, fiber integrity was associated with enhanced processing of positive emotion, but reduced interference from negative emotion.

To our knowledge, there are only few studies that have related specific fiber measures and clinical symptoms in alcoholism and HIV-1 infection. Although recent findings suggested the role of uncinate and cingulum in major depression (Zhang et al., 2012), in our study groups, we did not find exclusive relationships between cingulum and *uf* fiber integrity and emotion functions as tested with emotional word and face processing. Because the uncinate fasciculus connects the medial anterior temporal lobe ventrally including hippocampus and amygdala with medial and inferior orbitofrontal cortices, abnormalities in these regions may influence both attentional and emotional processing in patients with white matter abnormalities.

Even though the total study sample included 65 subjects, subgroup samples were relatively small, thereby limiting the interpretation of our results for population inference. Most of the HIV subjects had received HAART therapy, but a substantial proportion of subject had comorbidities including substance abuse other than alcohol, hepatitis, and depression further modifies HIV− and alcoholism-related effects on brain microstructure and associated

emotion and attention function. Thus, variability in fiber integrity measures and emotional processing may have been influenced by these comorbidities, which often occur in patients with HIV infection and alcoholism (Sassoon, Rosenbloom, Fama, Sullivan, & Pfefferbaum, 2012; Stubbe-Dräger et al., 2012; Wright, Heaps, Shimony, Thomas, & Ances, 2012). In addition, in vivo neuroimaging can only provide an approximate estimation of white matter fiber tract integrity. For example, in regions of complex tissue architecture, especially those with crossing fibers, axial diffusivity values can misrepresent underlying existent microstructural features of tissue organization (Wheeler-Kingshott and Cercignani, 2009; Klawiter et al., 2011). We used fiber-tracking algorithms developed to mitigate partial voluming effects from crossing fibers (Gerig et al., 2005; Rohlfing et al., 2010). Despite converging evidence for white matter compromise in HIV (Pfefferbaum et al., 2009; Müller-Oehring et al., 2010; Stubbe-Dräger et al., 2012) and alcoholism (Colrain et al., 2011; Konrad et al., 2012; Pfefferbaum, Rosenbloom, Rohlfing, & Sullivan, 2009; Schulte, Müller-Oehring, Pfefferbaum, & Sullivan, 2010), the specific role of association and commissural fiber tracts for the transmission and integration of emotional content in HIV and alcoholism needs further confirmation from future studies.

Together, our results indicate that individual variability in fiber integrity in alcoholism, HIV, and their comorbidity contributes to deficits in cognitive control processes and is reflected in enhanced attentional interference while processing emotional words and faces. These results highlight the functional relevance of association and commissural fiber tracts and their integrity in alcoholism and HIV infection to enable processing of emotional valence and selective attention.

Acknowledgments

This work was supported by National Institute on Alcohol Abuse and Alcoholism grants AA018022, AA017347, and AA017168. The authors thank Margaret J. Rosenbloom, M.A., for comments on this manuscript. We also thank Stephanie Sassoon, Ph.D., Megan Thompson, B.A., and Crystal Caldwell for help with recruiting and screening study participants and assistance in data collection. The information in this manuscript and the manuscript itself are new and original and has never been published either electronically or in print.

References

Adolphs R, Damasio H, Tranel D, Damasio AR. Cortical systems for the recognition of emotion in facial expressions. Journal for Neuroscience. 1996; 16:7678–7687.

American Psychiatric Association. Diagnostic and Statistical Manual of Mental Disorders. 4th Edition. American Psychiatric Press Inc.; Washington, DC: 2000. Text Revision (DSM-IV-TR)

Ances BM, Roc AC, Wang J, Korczykowski M, Okawa J, Stern J, Kim J, Wolf R, Lawler K, Kolson DL, Detre JA. Caudate blood flow and volume are reduced in HIV+ neurocognitively impaired patients. Neurology. 2006; 66:862–866. [PubMed: 16567703]

Ances BM, Ortega M, Vaida F, Heaps J, Paul R. Independent Effects of HIV, Aging, and HAART on Brain Volumetric Measures. Journal of Acquired Immune Deficiency Syndromes. 2012; 59:469–477. [PubMed: 22269799]

Bagasra O, Pomerantz RJ. Human immunodeficiency virus type 1 replication in peripheral blood mononuclear cells in the presence of cocaine. The Journal of Infectious Diseases. 1993; 168:1157–1164. [PubMed: 8228349]

Bannerman RL, Milders M, Sahraie A. Attentional bias to brief threat-related faces revealed by saccadic eye movements. Emotion. 2010; 10:733–738. [PubMed: 21038958]

Barnett KJ, Corballis MC. Speeded right-to-left information transfer: the result of speeded transmission in right-hemisphere axons? Neuroscience Letters. 2005; 380:88–92. [PubMed: 15854757]

Barrick TR, Lawes IN, Mackay CE, Clark CA. White matter pathway asymmetry underlies functional lateralization. Cerebral Cortex. 2007; 17:591–598. [PubMed: 16627859]

Basser PJ, Jones DK. Diffusion-tensor MRI: theory, experimental design and data analysis - a technical review. NMR in Biomedicine. 2002; 15:456–467. [PubMed: 12489095]

Basser PJ, Pierpaoli C. A simplified method to measure the diffusion tensor from seven MR images. Magnetic Resonance in Medicine. 1998; 39:928–934. [PubMed: 9621916]

Beck, AT.; Steer, RA.; Brown, GK. Manual for the Beck Depression Inventory-II. Psychological Corporation; San Antonio, TX: 1996.

Bodammer N, Kaufmann J, Kanowski M, Tempelmann C. Eddy current correction in diffusion-weighted imaging using pairs of images acquired with opposite diffusion gradient polarity. Magnetic Resonance in Medicine. 2004; 51:188–193. [PubMed: 14705060]

Borjabad A, Morgello S, Chao W, Kim SY, Brooks AI, Murray J, Potash MJ, Volsky DJ. Significant effects of antiretroviral therapy on global gene expression in brain tissues of patients with HIV-1-associated neurocognitive disorders. PLoS Pathogens. 2011; 7:e1002213. [PubMed: 21909266]

Boyadjieva NI, Sarkar DK. Role of microglia in ethanol's apoptotic action on hypothalamic neuronal cells in primary cultures. Alcoholism, Clinical and Experimental Research. 2010; 34:1835–1842.

Carretie L, Rios M, de la Gandara BS, Tapia M, Albert J, Lopez-Martin S, et al. The striatum beyond reward: caudate responds intensely to unpleasant pictures. Neuroscience. 2009; 164:1615–1622. [PubMed: 19778586]

Chang L, Wong V, Nakama H, Watters M, Ramones D, Miller EN, et al. Greater than age-related changes in brain diffusion of HIV patients after 1 year. Journal of Neuroimmune Pharmacology. 2008; 3:265–274. [PubMed: 18709469]

Clark US, Cohen RA, Westbrook ML, Devlin KN, Tashima KT. Facial emotion recognition impairments in individuals with HIV. Journal of the International Neuropsychological Society: JINS. 2010; 16:1127–1137. [PubMed: 20961470]

Colrain IM, Sullivan EV, Ford JM, Mathalon DH, McPherson SL, Roach BJ, Crowley KE, Pfefferbaum A. Frontally mediated inhibitory processing and white matter microstructure: age and alcoholism effects. Psychopharmacology. 2011; 213:669–679. [PubMed: 21161189]

Cooper CL, Cameron DW. Effect of alcohol use and highly active antiretroviral therapy on plasma levels of hepatitis C virus (HCV) in patients coinfected with HIV and HCV. Clinical Infectious Diseases. 2005; 41(Suppl 1):S105–109. [PubMed: 16265607]

Crovitz HF, Zener K. A group test for assessing hand- and eyedominance. The American Journal of Psychology. 1962; 75:271–276. [PubMed: 13882420]

Di Sclafani V, Mackay RD, Meyerhoff DJ, Norman D, Weiner MW, et al. Brain atrophy in HIV infection is more strongly associated with CDC clinical stage than with cognitive impairment. Journal of the International Neuropsychological Society: JINS. 1997; 3:276–287. [PubMed: 9161107]

Ernst T, Chang L, Jovicich J, Ames N, Arnold S. Abnormal brain activation on functional MRI in cognitively asymptomatic HIV patients. Neurology. 2002; 59:1343–1349. [PubMed: 12427881]

Etkin A, Egner T, Kalisch R. Emotional processing in anterior cingulate and medial prefrontal cortex. Trends in Cognitive Sciences. 2011; 15:85–93. [PubMed: 21167765]

Fama R, Rosenbloom MJ, Nichols BN, Pfefferbaum A, Sullivan EV. Working and episodic memory in HIV infection, alcoholism, and their comorbidity: baseline and 1-year follow-up examinations. Alcoholism, Clinical and Experimental Research. 2009; 33:1815–1824.

Fama R, Rosenbloom MJ, Sassoon SA, Thompson MA, Pfefferbaum A, et al. Remote semantic memory for public figures in HIV infection, alcoholism, and their comorbidity. Alcoholism, Clinical and Experimental Research. 2011; 35:265–276.

Fein G, Landman B, Tran H, McGillivray S, Finn P, Barakos J, et al. Brain atrophy in long-term abstinent alcoholics who demonstrate impairment on a simulated gambling task. Neuroimage. 2006; 32:1465–1471. [PubMed: 16872844]

Fortier CB, Leritz EC, Salat DH, Venne JR, Maksimovskiy AL, et al. Reduced cortical thickness in abstinent alcoholics and association with alcoholic behavior. Alcoholism, Clinical and Experimental Research. 2011; 35:2193–2201.

Gerig, G.; Corouge, I.; Vachet, C.; Krishnan, KR.; MacFall, JR. Quantitative analysis of diffusion properties of white matter fiber tracts: a validation study. 13th Proceedings of the International Society for Magnetic Resonance in Medicine; Miami, FL. 2005.

Gongvatana A, Cohen RA, Correia S, Devlin KN, Miles J, et al. Clinical contributors to cerebral white matter integrity in HIV-infected individuals. Journal of Neurovirology. 2011; 17:477–486. [PubMed: 21965122]

Gonzalez-Scarano F, Martin-Garcia J. The neuropathogenesis of AIDS. Nature reviews. Immunology. 2005; 5:69–81.

Goodkin K, Wilkie FL, Concha M, Asthana D, Shapshak P, et al. Subtle neuropsychological impairment and minor cognitive-motor disorder in HIV-1 infection. Neuroradiological, neurophysiological, neuroimmunological, and virological correlates. Neuroimaging Clinics of North America. 1997; 7:561–579. [PubMed: 9376968]

Hartikainen KM, Ogawa KH, Knight RT. Transient interference of right hemispheric function due to automatic emotional processing. Neuropsychologia. 2000; 38:1576–1580. [PubMed: 11074080]

Haruno M, Kuroda T, Doya K, Toyama K, Kimura M, et al. A neural correlate of reward-based behavioral learning in caudate nucleus: a functional magnetic resonance imaging study of a stochastic decision task. Journal for Neuroscience. 2004; 24:1660–1665.

Horvitz JC. Dopamine gating of glutamatergic sensorimotor and incentive motivational input signals to the striatum. Behavioural Brain Research. 2002; 137:65–74. [PubMed: 12445716]

Huang J, Chan RC, Gollan JK, Liu W, Ma Z, et al. Perceptual bias of patients with schizophrenia in morphed facial expression. Psychiatry Research. 2011; 185:60–65. [PubMed: 20646764]

Hutton HE, Lyketsos CG, Zenilman JM, Thompson RE, Erbelding EJ. Depression and HIV risk behaviors among patients in a sexually transmitted disease clinic. American Journal of Psychiatry. 2004; 161:912–914. [PubMed: 15121659]

Jackson MC, Wolf C, Johnston SJ, Raymond JE, Linden DE. Neural correlates of enhanced visual short-term memory for angry faces: an FMRI study. PLoS One. 2008; 3:e3536. [PubMed: 18958158]

Jenkinson, M. Improved unwarping of EPI volumes using regularized B0 maps. Paper presented at Seventh International Conference on Functional Mapping of the Human Brain; Brighton, UK. 2001.

Jenkinson M. A fast, automated, N-dimensional phase unwrapping algorithm. Magnetic Resonance in Medicine. 2003; 49:193–197. [PubMed: 12509838]

Johnson-Greene D, Adams KM, Gilman S, Junck L. Relationship between neuropsychological and emotional functioning in severe chronic alcoholism. Archives of Clinical Neuropsychology. 2002; 16:300–309.

Karnofsky DA, Abelmann WH, Craver LF, Burchenal JH. The use of the nitrogen mustards in the palliative treatment of carcinoma. With particular reference to bronchogenic carcinoma. Cancer. 1948; 1:634–656.

Kim DH, Adalsteinsson E, Glover GH, Spielman DM. Regularized higher-order in vivo shimming. Magnetic Resonance in Medicine. 2002; 48:715–722. [PubMed: 12353290]

Kim S, Lee D. Prefrontal cortex and impulsive decision making. Biological Psychiatry. 2011; 69:1140–1146. [PubMed: 20728878]

Klawiter EC, Schmidt RE, Trinkaus K, Liang HF, Budde MD, Naismith RT, Song SK, Cross AH, Benzinger TL. Radial diffusivity predicts demyelination in ex vivo multiple sclerosis spinal cords. Neuroimage. 2011; 55:1454–1460. [PubMed: 21238597]

Koob GF. Theoretical Frameworks and Mechanistic Aspects of Alcohol Addiction: Alcohol Addiction as a Reward Deficit Disorder. Current Topics in Behavioral Neurosciences. Jul 10.2011 Epub ahead of print.

Konrad A, Vucurevic G, Lorscheider M, Bernow N, Thümmel M, Chai C, Pfeifer P, Stoeter P, Scheurich A, Fehr C. Broad disruption of brain white matter microstructure and relationship with neuropsychological performance in male patients with severe alcohol dependence. Alcohol and Alcoholism. 2012; 47:118–126. [PubMed: 22214998]

Kumar A, Cook IA. White matter injury, neural connectivity and the pathophysiology of psychiatric disorders. Developmental Neuroscience. 2002; 24:255–261. [PubMed: 12457063]

Kumar AM, Ownby RL, Waldrop-Valverde D, Fernandez B, Kumar M. Human immunodeficiency virus infection in the CNS and decreased dopamine availability: relationship with

neuropsychological performance. Journal of Neurovirology. 2011; 17:26–40. [PubMed: 21165787]

Laubenberger J, Häussinger D, Bayer S, Thielemann S, Schneider B, et al. HIV-related metabolic abnormalities in the brain: depiction with proton MR spectroscopy with short echo times. Radiology. 1996; 199:805–810. [PubMed: 8638009]

Loy DN, Kim JH, Xie M, Schmidt RE, Trinkaus K, Song SK. Diffusion tensor imaging predicts hyperacute spinal cord injury severity. Journal of Neurotrauma. 2007; 24:979–990. [PubMed: 17600514]

Makris N, Oscar-Berman M, Jaffin SK, Hodge SM, Kennedy DN, et al. Decreased volume of the brain reward system in alcoholism. Biological Psychiatry. 2008; 64:192–202. [PubMed: 18374900]

Marinkovic K, Oscar-Berman M, Urban T, O'Reilly CE, Howard JA, et al. Alcoholism and dampened temporal limbic activation to emotional faces. Alcoholism: Clinical & Experimental Research. 2009; 33:1880–1892.

Martin EM, Nixon H, Pitrak DL, Weddington W, Rains NA, et al. Characteristics of prospective memory deficits in HIV-seropositive substance-dependent individuals: preliminary observations. Journal of Clinical and Experimental Neuropsychology. 2007; 29:496–504. [PubMed: 17564915]

Mori S, Zhang J. Principles of diffusion tensor imaging and its applications to basic neuroscience research. Neuron. 2006; 51:527–539. [PubMed: 16950152]

Mori S, van Zijl PC. Fiber tracking: principles and strategies — a technical review. NMR in Biomedicine. 2002; 15:468–480. [PubMed: 12489096]

Müller-Oehring EM, Schulte T, Rosenbloom MJ, Pfefferbaum A, Sullivan EV. Callosal degradation in HIV-1 infection predicts hierarchical perception: a DTI study. Neuropsychologia. 2010; 48:1133–1143. [PubMed: 20018201]

Neeman M, Freyer JP, Sillerud LO. A simple method for obtaining cross-term-free images for diffusion anisotropy studies in NMR microimaging. Magnetic Resonance in Medicine. 1991; 21:138–143. [PubMed: 1943671]

Nelson, HE. National Adult Heading Test (NART): Test Manual. NFER-Nelson; Windsor: 1982.

Pandya, DN.; Seltzer, B. The topography of commissural fibers. In: Lepore, F.; Ptito, M.; Jasper, HH., editors. Two hemispheres—one brain: functions of the corpus callosum. Wiley; New York: 1986. p. 47-73.

Persidsky Y, Zheng J, Miller D, Gendelman HE. Mononuclear phagocytes mediate blood-brain barrier compromise and neuronal injury during HIV-1-associated dementia. Journal of Leukocyte Biology. 2000; 68:413–422. [PubMed: 10985259]

Persidsky Y, Ho W, Ramirez SH, Potula R, Abood ME, et al. HIV-1 infection and alcohol abuse: neurocognitive impairment, mechanisms of neurodegeneration and therapeutic interventions. Brain, Behavior, and Immunity. 2011; 25(Suppl 1):S61–70.

Pfefferbaum A, Rosenbloom M, Crusan K, Jernigan TL. Brain CT changes in alcoholics: effects of age and alcohol consumption. Alcoholism: Clinical & Experimental Research. 1988; 12:81–87.

Pfefferbaum A, Rosenbloom MJ, Rohlfing T, Kemper CA, Deresinski S, et al. Frontostriatal fiber bundle compromise in HIV infection without dementia. AIDS. 2009; 23:1977–1985. [PubMed: 19730350]

Pfefferbaum A, Rosenbloom MJ, Fama R, Sassoon SA, Sullivan EV. Transcallosal white matter degradation detected with quantitative fiber tracking in alcoholic men and women: selective relations to dissociable functions. Alcoholism: Clinical & Experimental Research. 2010; 34:1201–1211.

Pfefferbaum A, Rosenbloom M, Rohlfing T, Sullivan EV. Degradation of association and projection white matter systems in alcoholism detected with quantitative fiber tracking. Biological Psychiatry. 2009; 65:680–690. [PubMed: 19103436]

Pfefferbaum A, Rosenbloom MJ, Sassoon SA, Kemper CA, Deresinski S, et al. Regional Brain Structural Dysmorphology in Human Immunodeficiency Virus Infection: Effects of Acquired Immune Deficiency Syndrome, Alcoholism, and Age. Biological Psychiatry. Mar 26.2012 Epub ahead of print.

Pierpaoli C, Basser PJ. Toward a quantitative assessment of diffusion anisotropy. Magnetic Resonance in Medicine. 1996; 36:893–906. [PubMed: 8946355]

Potula R, Haorah J, Knipe B, Leibhart J, Chrastil J, et al. Alcohol abuse enhances neuroinflammation and impairs immune responses in an animal model of human immunodeficiency virus-1 encephalitis. American Journal of Pathology. 2006; 168:1335–1344. [PubMed: 16565506]

Rochat L, Billieux J, Van der Linden M. Difficulties in disengaging attentional resources from self-generated thoughts moderate the link between dysphoria and maladaptive self-referential thinking. Cognition & Emotion. Oct 5.2011 Epub ahead of print.

Rohlfing T, Maurer CR Jr. Nonrigid image registration in shared-memory multiprocessor environments with application to brains, breasts, and bees. IEEE Transactions on Information Technology in Biomedicine. 2003; 7:16–25. [PubMed: 12670015]

Rohlfing T, Zahr NM, Sullivan EV, Pfefferbaum A. The SRI24 multichannel atlas of normal adult human brain structure. Human Brain Mapping. 2010; 31:798–819. [PubMed: 20017133]

Rosenbloom M, Sullivan EV, Pfefferbaum A. Using magnetic resonance imaging and diffusion tensor imaging to assess brain damage in alcoholics. Alcohol Research & Health. 2003; 27:146–152. [PubMed: 15303625]

Salloum JB, Ramchandani VA, Bodurka J, Rawlings R, Momenan R, et al. Blunted rostral anterior cingulate response during a simplified decoding task of negative emotional facial expressions in alcoholic patients. Alcoholism: Clinical & Experimental Research. 2006; 31:1490–1504.

Sassoon SA, Rosenbloom MJ, Fama R, Sullivan EV, Pfefferbaum A. Selective neurocognitive deficits and poor life functioning are associated with significant depressive symptoms in alcoholism-HIV infection comorbidity. Psychiatry Research. 2012 Epub ahead of print.

Schulte T, Mueller-Oehring EM, Rosenbloom MJ, Pfefferbaum A, Sullivan EV. Differential effect of HIV infection and alcoholism on conflict processing, attentional allocation, and perceptual load: evidence from a Stroop Match-to-Sample task. Biological Psychiatry. 2005; 57:67–75. [PubMed: 15607302]

Schulte T, Müller-Oehring EM, Javitz H, Pfefferbaum A, Sullivan EV. Callosal Compromise Differentially Affects Conflict Processing and Attentional Allocation in Alcoholism, HIV, and Their Comorbidity. Brain Imaging and Behavior. 2008; 2:27–38. [PubMed: 19360136]

Schulte T, Müller-Oehring EM, Pfefferbaum A, Sullivan EV. Neurocircuitry of emotion and cognition in alcoholism: contributions from white matter fiber tractography. Dialogues in Clinical Neuroscience. 2010; 12:554–560. [PubMed: 21319499]

Schulte T, Müller-Oehring EM, Rohlfing T, Pfefferbaum A, Sullivan EV. White matter fiber degradation attenuates hemispheric asymmetry when integrating visuomotor information. Journal of Neuroscience. 2010; 30:12168–12178. [PubMed: 20826679]

Schulte T, Müller-Oehring EM, Sullivan EV, Pfefferbaum A. Disruption of Emotion and Conflict Processing in HIV Infection with and without Alcoholism Comorbidity. Journal of the International Neuropsychological Society: JINS. 2011; 22:1–14. [PubMed: 21418720]

Schulte T, Müller-Oehring EM, Sullivan EV, Pfefferbaum A. Synchrony of corticostriatal-midbrain activation enables normal inhibitory control and conflict processing in recovering alcoholic men. Biological Psychiatry. 2012; 71:269–278. [PubMed: 22137506]

Seo H, Barraclough DJ, Lee D. Lateral intraparietal cortex and reinforcement learning during a mixed-strategy game. Journal of Neuroscience. 2009; 29:7278–7289. [PubMed: 19494150]

Silveri MM, Rohan ML, Pimentel PJ, Gruber SA, Rosso IM, et al. Sex differences in the relationship between white matter microstructure and impulsivity in adolescents. Magnetic Resonance Imaging. 2006; 24:833–841. [PubMed: 16916700]

Song SK, Sun SW, Ramsbottom MJ, Chang C, Russell J, et al. Dysmyelination revealed through MRI as increased radial (but unchanged axial) diffusion of water. Neuroimage. 2002; 17:1429–1436. [PubMed: 12414282]

Song SK, Sun SW, Ju WK, Lin SJ, Cross AH, Neufeld AH. Diffusion tensor imaging detects and differentiates axon and myelin degeneration in mouse optic nerve after retinal ischemia. Neuroimage. 2003; 20:1714–1722. [PubMed: 14642481]

Stout JC, Ellis RJ, Jernigan TL, Archibald SL, Abramson I, et al. Progressive cerebral volume loss in human immunodeficiency virus infection: a longitudinal volumetric magnetic resonance imaging study. HIV Neurobehavioral Research Center Group. Archives of Neurology. 1998; 55:161–168. [PubMed: 9482357]

Stubbe-Dräger B, Deppe M, Mohammadia S, Keller SS, Kugel H, Gregor N, Evers S, Young P, Ringelstein EB, Arendt G, Knecht S, Husstedt IW. Early microstructural white matter changes in patients with HIV: a diffusion tensor imaging study. BMC Neurology. 2012; 12:23. [PubMed: 22548835]

Sun SW, Liang HF, Trinkaus K, Cross AH, Armstrong RC, et al. Noninvasive detection of cuprizone induced axonal damage and demyelination in the mouse corpus callosum. Magnetic Resonance in Medicine. 2009; 55:302–308. [PubMed: 16408263]

Towgood KJ, Pitkanen M, Kulasegaram R, Fradera A, Kumar A, Soni S, Sibtain NA, et al. Mapping the brain in younger and older asymptomatic HIV-1 men: frontal volume changes in the absence of other cortical or diffusion tensor abnormalities. Cortex. 2012; 48:230–241. [PubMed: 21481856]

Wang JJ, Durazzo TC, Gazdzinski S, Yeh PH, Mon A, et al. MRSI and DTI: a multimodal approach for improved detection of white matter abnormalities in alcohol and nicotine dependence. NMR in Biomedicine. 2009; 22:516–522. [PubMed: 19156697]

Wang H, Sun J, Goldstein H. Human immunodeficiency virus type 1 infection increases the in vivo capacity of peripheral monocytes to cross the blood-brain barrier into the brain and the in vivo sensitivity of the blood-brain barrier to disruption by lipopolysaccharide. Journal of Virology. 2008; 82:7591–7600. [PubMed: 18508884]

Wheeler-Kingshott CA, Cercignani M. About “axial” and “radial” diffusivities. Magnetic Resonance in Medicine. 2009; 61:1255–1260. [PubMed: 19253405]

Williams JM, Mathews A, MacLeod C. The emotional Stroop task and psychopathology. Psychological Bulletin. 1996; 120:3–24. [PubMed: 8711015]

Wright PW, Heaps JM, Shimony JS, Thomas JB, Ances BM. The Effects of HIV and combination antiretroviral therapy on white matter integrity. AIDS. 2012 Epub ahead of print.

Xu D, Mori S, Solaiyappan M, van Zijl PC, Davatzikos C. A framework for callosal fiber distribution analysis. Neuroimage. 2002; 17:1131–1143. [PubMed: 12414255]

Xue R, van Zijl PC, Crain BJ, Solaiyappan M, Mori S. In vivo three-dimensional reconstruction of rat brain axonal projections by diffusion tensor imaging. Magnetic Resonance in Medicine. 1999; 42:1123–1127. [PubMed: 10571934]

Yin X, Han Y, Ge H, Xu W, Huang R, et al. Inferior frontal white matter asymmetry correlates with executive control of attention. Human Brain Mapping. Nov 23.2011 Epub ahead of print.

Zhang A, Leow A, Ajilore O, Lamar M, Yang S, et al. Quantitative tract-specific measures of uncinate and cingulum in major depression using diffusion tensor imaging. Neuropsychopharmacology. 2012; 37:959–967. [PubMed: 22089322]

HIGHLIGHTS

- A substantial proportion of individuals with HIV have comorbid conditions, notably alcohol abuse.
- Alcoholism (ALC) and HIV was associated with compromise in emotion and attention processes.
- In HIV, uncinate fiber compromise correlated with enhanced interference from negative emotion.
- In ALC and ALC+HIV, poorer callosal integrity was related to enhanced emotional interference.
- Fiber integrity in ALC and HIV has functional relevance for emotion and attention processing.

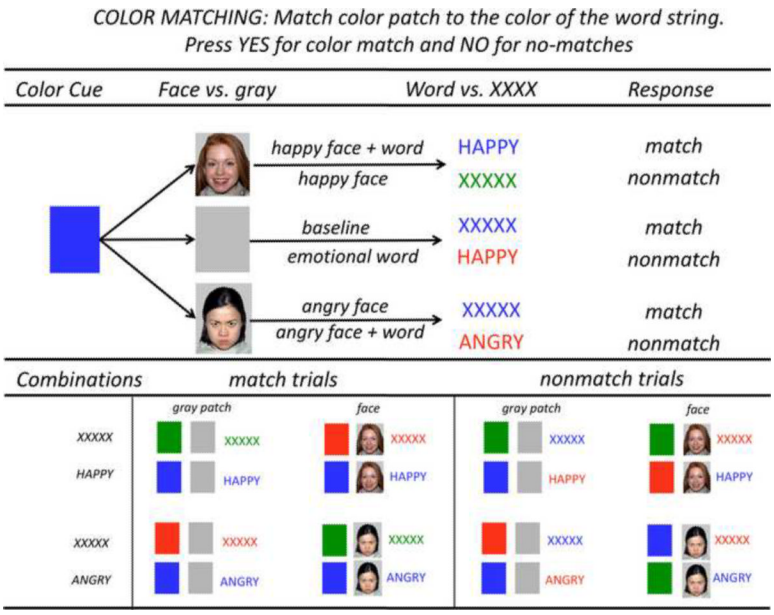

Figure 1. Emotional Stroop Paradigm

The task was to match the color of a *color cue* to that of a *target* stimulus (word or XXXXX) by pressing a YES-key for color matches and a NO-key for color nonmatches. The task had the following *color matching* conditions: 1) no face–letter string (baseline); 2) no face–word HAPPY; 3) no face–word ANGRY; 4) happy face–letter string; 5) angry face–letter string; 6) happy face–word HAPPY; 7) angry face–word ANGRY. Face stimuli were selected from the MacBrain Face Stimulus Set (http://www.macbrain.org/resources.htm). Development of the MacBrain Face Stimulus Set was overseen by Nim Tottenham and supported by the John D. and Catherine T. MacArthur Foundation Research Network on Early Experience and Brain Development.

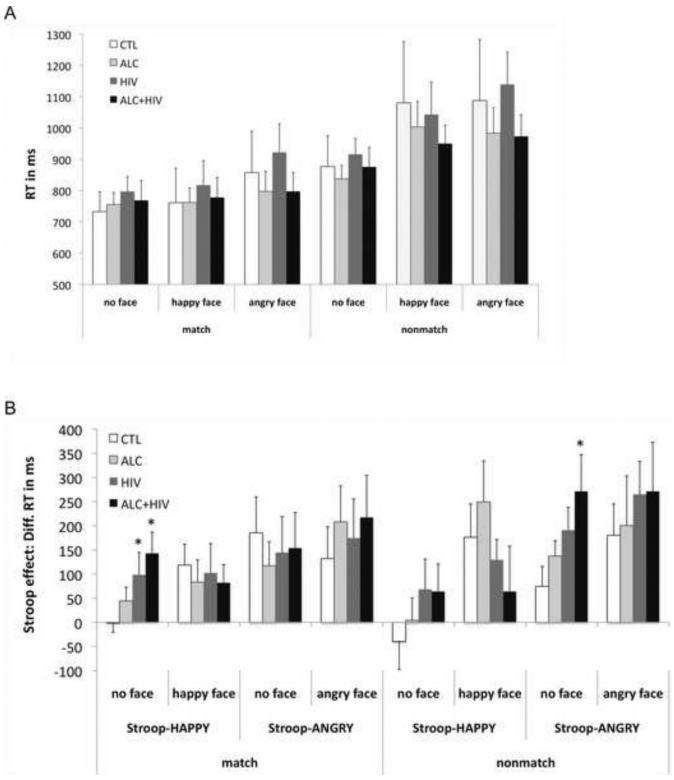

Figure 2. Behavioral results

A. Mean reaction times (RT) and standard error bars for matching colors between cue and letter string (XXXXX) (baseline) for color-matches and nonmatches, trials without and with faces (happy and angry), for each study group: healthy controls (CTL), patients with alcoholism (ALC), HIV infection (HIV) and comorbid disorder (ALC+HIV). Note that baseline color-matching RTs for each condition did not significantly differ between groups. **B.** Emotional Stroop effects: Difference RTs between word trials and baseline trials for the Stroop words HAPPY and ANGRY, for trials with and without emotional faces for each study group, and separately for match and nonmatch trials.

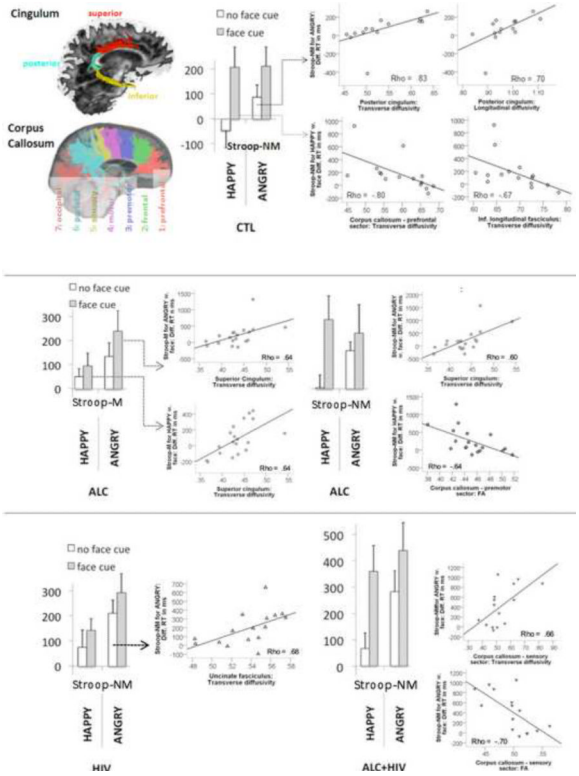

Figure 3. Structure-function relationships

Correlations between emotional Stroop effects and fiber integrity measures for each study group: healthy controls (CTL), patients with alcoholism (ALC), HIV infection (HIV), and comorbid disorder (ALC+HIV).

Table 1

Demographic data (mean ± S.D.) and statistical results for four groups: Healthy control subjects, and patients with alcoholism, HIV-1 infection, and those with both diseases.

	Controls (CTL)	Alcoholism (ALC)	HIV− infection	HIV+ Alcoholism	χ^2, *F*, *t value*	*p*
n	*15*	*19*	*16*	*15*		
Sex (women/men)	6/9	10/9	4/12	5/10	3.02[a]	.39
Ethnicity (n)					11.23[a]	.08
Asian	3	0	0	0		
African-american / black	7	8	8	7		
Pacific islander	0	0	0	0		
Caucasian / white	5	11	8	8		
Hispanic [d]	0	2	2	4		
Age (years)	42 (12.2)	46 (11.8)	51 (7.3)	46 (10)	2.00[b]	.12
Education (years)	14.6 (2)	13.6 (2.8)	14 (2.7)	12.8 (2.2)	1.38[b]	.26
Verbal IQ (NART)	111 (10.1)	107 (9.6)	108 (9.6)	105 (7.9)	.91[b]	.44
Lifetime alcohol consumption (kg)	23 (38)	898 (639)	54 (56)	759.7 (696)	14.61[b]	**.0001** *ALC+HIV = ALC > HIV =CTL*
Alcohol abstinence prior to the study (months)	-	19.3 (29)	-	13.4 (27)	.63[c]	.54
CD4 (cell/mm^3)	-	-	556.3 (278)	407.7 (162)	1.80[c]	.08
Age ALC onset (years)	-	23 (9)	-	20 (6)	.96[c]	.34
Age HIV onset (years)	-	-	36 (7)	32 (10)	1.50[c]	.14
HART medication (n)	-	-	13	13	.17[a]	.68
Body Mass Index	25.8 (5.1)	27.3 (3.8)	24.5 (3.0)	25.1 (3.8)	1.67[b]	.18
Karnofski score (0–100)	100 (0)	100 (0)	99.4 (2.5)	98.7 (3.5)	1.21[b]	.31
GAF score (1–100) – Global Functioning	84 (5.2)	72 (10.8)	73 (10.7)	67 (7.7)	9.56[b]	**.0001** *ALC, HIV, ALC+HIV < CTL*
BDI[e] score	2.7 (2.5)	6.3 (4.1)	9.3 (8.6)	8.9 (7.7)	3.57[b]	**.019** *HIV, ALC+HIV > CTL*
Other co-morbidity (n)	0	7	4	10		

	Controls (CTL)	Alcoholism (ALC)	HIV− infection	HIV+ Alcoholism	χ^2 , *F, t value*	*p*
Hepatitis C	0	0	3	6	13.8[a]	**.003**
Other substance abuse	0	5	0	4	9.53[a]	**.023**
Smoking (past/current)	0/1	2/8	2/3	1/7	11.3[a]	.078
SCID mood diagnosis:					3.06[a]	.38
Anxiety (past/current)	0/0	3/0	2/1	3/0		
Depression (past/current)	0/0	5/2	3/0	5/0		

[a]Pearson χ^2;

[b]univariate ANOVA: *F* value;

[c]independent samples T-test: *t* value

[d]Hispanic participants are included in ethnic categories above

[e]Beck Depression Inventory (BDI-II) (Beck, Steer, & Brown 1996)

Table 2

Group differences (*F, p*-values) for DTI-based fiber integrity measures: fractional anisotropy (FA), transverse (λt) and longitudinal (λl) diffusivity.

Fiber Tract		FA			λ *t*			λl	
		F	***p***	***posthoc***	***F***	***p***	***posthoc***	***F***	***p***
slf		.49	*ns*		.34	*ns*		.47	*ns*
ilf		***4.07***	***.01***	HIV, ALC+HIV < CTL	.88	*ns*		.21	*ns*
uf		***3.48***	***.02***	ALC, HIV, ALC+HIV < CTL	***3.10***	***.03***	HIV, ALC+HIV > CTL	.66	*ns*
c	***s***	1.04	*ns*		1.02	*ns*		1.12	*ns*
	p	.55	*ns*		.45	*ns*		1.08	*ns*
	i	.60	*ns*		.33	*ns*		1.28	*ns*
cc	***1***	.83	*ns*		1.38	*ns*		1.40	*ns*
	2	2.05	*ns*		.61	*ns*		.23	*ns*
	3	1.38	*ns*		1.30	*ns*		1.01	*ns*
	4	.29	*ns*		.32	*ns*		.31	*ns*
	5	1.33	*ns*		.58	*ns*		.27	*ns*
	6	.38	*ns*		.67	*ns*		.80	*ns*
	7	.49	*ns*		.51	*ns*		.48	*ns*

c, cingulum (s=superior, p=posterior, i=inferior); slf, superior longitudinal fasciculus; ilf, inferior longitudinal fasciculus; uf, uncinate fasciculus; cc, corpus callosum sectors: (1 =prefrontal, 2=frontal, 3=premotor, 4=motor, 5=sensory, 6=parietal, 7=occipital).

Table 3

Spearman Rho correlation fiber integrity measures (FA, λt, λl) and emotional Stroop conflict for each study group (CTL, ALC, HIV, ALC+HIV), 2-tailed; $p_{\text{Bonferroni corr.}}$<.007 in bold.

A. Cortico-limbic fiber tracts

	Stroop effect		Fiber		FA		λt		λl	
	Attention	**Emotion**	**Face**		***rho***	***p***	***rho***	***p***	***rho***	***p***
CTL	NM	A	−	*pc*			**.83**	**.0001**	**.70**	**.003**
		H	+	*sc*	.65	.008				
				ilf			**−.67**	**.006**		
				cc1	.65	.008	**−.80**	**.0001**	**−.75**	**.001**
				cc2	**.69**	**.004**	−.65	.009	**−.68**	**.005**
				cc3	**.66**	**.007**				
				cc5			**−.67**	**.006**		
ALC	M	A	+	*sc*	**−.59**	**.007**	**.64**	**.003**		
		H	+	*sc*	−.59	.008	**.64**	**.003**		
	NM	A	+	*sc*			**.60**	**.007**		
				cc3	**−.68**	**.001**				
		H	+	*cc3*	**−.64**	**.003**				
HIV	NM	A	−	*uf*			**.68**	**.004**		
ALC+HIV	NM	A	+	*cc5*	**−.70**	**.004**	.66	.008		

Abbreviations Fiber tracts: slf, superior longitudinal fasciculus; ilf, inferior longitudinal fasciculus; sc, superior cingulum; pc, posterior cingulum; ic, inferior cingulum; uf, uncinate fasciculus; pct, pontocerebellar tract; callosal sectors; ccl=prefrontal, cc2=frontal, cc3=premotor, cc4=motor, cc5=sensory, cc6=parietal, cc7=occipital; Attention: M=match, NM=nonmatch; Emotion: H=happy, A=angry; Face: +(yes), − (no).

Table 4

Statistical relationship between fiber integrity measures (FA, λt, λl), demographic and clinical variables for each study group (CTL, ALC, HIV, ALC +HIV); Spearman Rho correlation, 1-tailed; $p_{\text{Bonferroni corr.}} < .014$.

	Variable	Fiber	FA		λt		λl	
			rho	p	rho	p	rho	p
CTL	*age*	*ilf*			.60	.009	.60	.009
ALC	*age*	*ilf*	−.69	.001	.81	.0001	.77	.0001
		sc					.63	.002
		uf			.54	.009		
		ccl	−.52	.011	.58	.005		
	BDI	*ccl*	−.56	.008				
HIV	*processing speed*	*cc5*	−.64	.004				
	# *errors*	*uf*					.62	.005
ALC+HIV	*days abstinent*	*cc6*	.57	.013				
	processing speed	*cc3*			.58	.012		
		cc5			.56	.014	.59	.011
	# *errors*	*slf*					.64	.005

sc, superior cingulum; pc, posterior cingulum; ic, inferior cingulum; uf, uncinate fasciculus; pct, pontocerebellar tract; callosal sectors; ccl=prefrontal, cc2=frontal, cc3=premotor, cc4=motor, cc5=sensory, cc6=parietal, cc7=occipital.